DEPOSITION OF NANOSILVER-ORGANOSILICON COMPOSITE FILMS USING AN ATMOSPHERIC PRESSURE DC PLASMA JET[*]

X. DENG[1,2], A. YU NIKIFOROV[1,3], P. VANRAES[1], C. LEYS[1]

[1] Ghent University, Department of Applied Physics, Sint-Pietersnieuwstraat 41, 9000, Ghent, Belgium,
E-mail: xiaolong.deng@ugent.be
[2] National University of Defense Technology, College of Optoelectric Science and Engineering,
Changsha, 410073, Hunan, China
[3] Institute of Solution Chemistry RAS, Academicheskayastr, 1, 153045, Ivanovo, Russia

Abstract. Silver nanoparticles embraced hybrid thin films were deposited by an atmospheric pressure direct current plasma jet system using tetramethyldisiloxane as organosilicon precursor. Nanoparticles were directly introduced into the process. The characterization of the hybrid films was investigated using XPS and radio frequency glow discharge optical emission spectroscopy (RF-GD-OES). It was found that composite films with Ag-NPs can be deposited by our method with the silver content in the film up to 50%.

Key words: silver nanoparticles, thin film, plasma deposition, glow discharge optical emission spectroscopy.

1. INTRODUCTION

It is well-known that infections associated with medical devices are responsible for substantial morbidity and cause a steep cost increase in healthcare [1]. Implanted devices cause especially massive infections. An essential event in the initiation of an infection related to biomaterials is microbial adhesion to the device. Often, bacteria get attached to the patient-derived glycoprotein coating which begins to deposit immediately after implantation on most devices. The microbial adhesion to the surface followed by cell growth and colonization results in the formation of a biofilm, which is capable of shielding the underlying micro-organisms from antimicrobials, chemical biocides and host defense mechanisms [2].

---

[*] Paper presented at the 16th International Conference on Plasma Physics and Applications, June 20–25, 2013, Magurele, Bucharest, Romania.

Therefore, biofilm prevention attracts substantial interest. The development of anti-adhesive or anti-microbial materials is highly valuable for biomedical applications.

As a broad-spectrum antimicrobial agent, silver is increasingly used in medical products. The release of silver ions is believed to be one of the reasons for its antibacterial properties [3]. It was proposed that ionic silver strongly interacts with thiol groups of enzymes, causing structural changes that lead to disruption of metabolic processes, followed by cell death. Due to the large surface-to-volume ratio, silver nanoparticles (Ag-NPs) release increased Ag^+ when compared to bulk silver surface.

Polymers or thin films embodying Ag-NPs, which have attracted substantial effort, may represent a feasible way to control the rate of silver release and provide long lasting antimicrobial properties. Various methods have been investigated to fabricate the hybrid surfaces. In general, the strategies of the methods can be classified into two major groups according to the mechanism of the generation.

The first group of strategies implants or grafts the Ag-NPs on the topmost surface of substrates by immersing them into a silver solution or Ag-NP dispersion [4–7]. To enhance the efficiency of incorporation, certain techniques, such as UV radiation and plasma treatment, are introduced to the process. N. K. Vu *et al.* have deposited three different size Ag-NPs onto polyamide 6,6 (PA) fabric pre-treated using air dielectric barrier discharge (DBD) plasma [4]. The DBD treatment on PA induced a threefold increase in Ag adsorption. L. Zhao *et al.* reported the fabrication of Ti implants incorporated with Ag-NPs [5]. The Ag-NPs shows tightly adhesion to the wall of titanium nanotubes prepared by immersion in a silver nitrate solution followed by UV light radiation. Although various sizes of Ag-NPs were implanted using proper silver solutions and dispersions, the substrates typically contained less than 2% of silver which limited the antibacterial period.

The second group of strategies implements the deposition of Ag-NP embodying hybrid thin films on substrates. The hybrid films have been deposited using various techniques, such as plasma-enhanced chemical vapor deposition (PE-CVD) [2, 3, 8-10], plasma spraying deposition [11] and casting or spin coating [12]. C. Saulou *et al.* synthesized nanosilver-organosilicon composite films by combining the plasma deposition and sputtering process in a vacuum chamber [2]. The silver content, various from few percent to 32.5%, was controlled by discharge parameters, such as discharge power, bias voltage and partial pressure of the precursor. The films exhibited anti-adhesive potentialities toward the model yeast Saccharomyces cerevisiae.

In this work, silver nanoparticles embraced hybrid thin films have been deposited by an atmospheric pressure direct current plasma jet system using tetramethyldisiloxane (TMDSO) as organosilicon precursor. Silver nanoparticles were introduced to the deposition process by a direct nanoparticles feeding system. The hybrid films were characterized using X-ray photoelectron spectroscopy (XPS) and radio frequency glow discharge optical emission spectroscopy (RF-GD-OES).

2. EXPERIMENTAL SECTION

Figure 1 shows the schematic of the plasma deposition system which is similar to our system described in [13]. An atmospheric pressure DC plasma jet, which consists of a pin-to-mesh electrode in a quartz tube, is used as the plasma source. The pin cathode, which is manufactured from a 2 mm tungsten rod with a conically sharpened tip, is connected to the negative polarity of a direct current high voltage power supply (Technix SR, France) through a ballast resistor. The mesh, 10 mm away from the pin, is placed at the outlet of the tube as it was done in [13].

The Si wafer substrate of 7 mm × 7 mm size is placed 10 mm away from the nozzle of the jet in order to avoid overheating due to plasma and still have high flux of active species on the surface of substrate. Nitrogen is the working gas for the plasma jet. By passing nitrogen through a bubble system, the organosilicon precursor TMDSO is vaporized. In order to prevent possible formation of microparticles in the gas phase, the diluting gas for the precursor is limited to 5 sccm (standard cubic centimeter per minute). Oxygen at a flow rate of 100 sccm is added to promote the conversion of the monomer. Ag-NPs (100 nm, Sigma-Aldrich, Belgium) are provided by a designed container and introduced into the process by the passing nitrogen. Gases from the 4 channels run into a cylindrical mixer and flow to the plasma jet. The total gas flow of the jet is maintained at 7000 sccm. The plasma is sustained at a discharge power of 22.5W. According to our previous results [13], the deposition rate of the thin films is 352 nm/min. each samples is prepared with 2 minutes of plasma exposure time. The deposition is carried out at various flow rate of the feed gas through the Ag-NPs container.
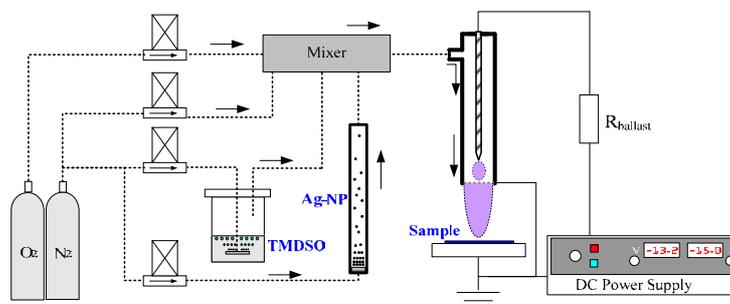

Fig. 1 – Schema of the experimental set-up for the plasma deposition process.

X-ray photoelectron spectroscopy (XPS) for surface characterization of deposited films are performed on a Versaprobe II system (Physical Electronics (PHI), USA) equipped with a monochromatic Al Kα X-ray source ($h\nu$ = 1486.6 eV). The power of this source is set to 23.3 W. The pressure in the analyzing chamber is maintained below 10^{-7} Pa during analysis and the diameter of the

analyzed area is 100 μm. Survey (0–1100 eV) are recorded at a pass energy of 117.4 eV. XPS analyses are performed with a take-off angle of 45° relatively to the sample surface. The value of 285 eV of the hydrocarbon C1s core level is used as a calibration of the energy scale.
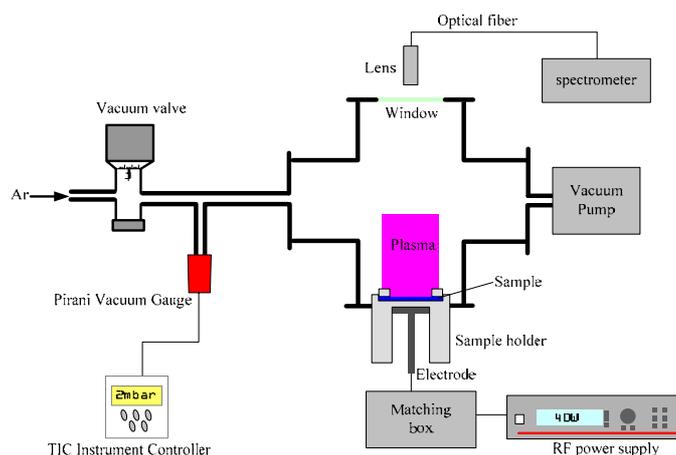

Fig. 2 – Schematic diagram of the experimental set-up for RF-GD-OES.

Glow discharge optical emission spectroscopy (GD-OES) for the analysis of quantification and depth profile is performed on a Grimm-type glow discharge source with a radio frequency (RF) power supply (Advanced Energy Cesar, USA). The scheme of the GD-OES setup is shown in Fig. 2. Argon is used as working gas. After introducing a sample to the sample stage, the chamber is pumped to 10^{-3} mbar and then flushed by argon for 3 min to eliminate the background gases. The plasma is generated in 2 mbar argon atmosphere at a power of 40W. The emission spectra are collected by a spectrometer (Ocean Optics S2000, USA) with a resolution of 0.2 nm.

3. RESULTS AND DISCUSSION

3.1. XPS MEASUREMENTS

As known, plasma film deposition starts with chain breaking and dissociation of monomer molecules of the precursor and thereby creating radicals. These radicals recombine with each other, form cross-linking structures and finally are deposited on the substrate. In the present study we, used a mixture of TMDSO with O_2 resulting in the composition of the film close to inorganic SiO_2. In our previous work, it was shown by XPS and FTIR measurements that deposited films without

Ag-NPs consists of < 55% of O at an O_2 flow rate of 100 sccm. High resolution XPS spectra shown that the films consist of $(CH_3)_xSiO_y$ ($x = 1,2$) groups (up to 25%), CH_3SiO_3 groups of low concentration of 11% and a high amount of SiO_4 groups (< 64%). The deposition rate can be controlled by the oxygen content in the feed gas and can be varied from 172 nm/min (no O_2) up to 450 nm/min (100 sccm O_2) due to effective monomer decomposition by the plasma. In agreement with our previous research, the amount of O_2 has been fixed at 100 sccm in order to achieve the highest deposition rate, but still to suppress possible nucleation in the gas phase. In previous experiments we observed formation of white micro-particles on the surface of the deposited film at an O_2 concentration in the feed gas higher than 100 sccm.

In the present work we have focused on the possibility of one step dry process of composite film deposition with a high amount on Ag-NPs incorporated into the film. One of the challenging tasks is a deposition of uniform films with the suppression of micro-particles growth in the gas phase. For the film without incorporation of Ag-NPs it has been achieved in our work [13] by optimization of the deposition process in terms of gas composition and the discharge power. The second issue about the experiments is the use of proper analytical techniques for analysis of the deposited films. At the first stage we used the XPS method in order to carry out identification and quantification of the chemical composition of the deposited films.

Table 1

Atomic percentage of a control sample and a hybrid sample

sample	O (%)	C (%)	Si (%)	Ag (%)
A control sample	48	28	24	0
A hybrid sample	45.3	24.8	25.6	4.3

Low-resolution XPS survey spectra are acquired to reveal information on the relative amounts of elements present in the films. The XPS results and the XPS spectra for two samples (a control sample without Ag-NPs and a sample with carrying gas flow rate of 1000 sccm) are shown in Table 1 and Fig. 3 respectively. As shown in Fig. 3, the survey spectrum indicates that oxygen (O), carbon (C) and silicon (Si) are present in the film for a control sample deposited without Ag-NPs in the process.

In contrast, when the Ag-NPs are introduced into the deposition process, the Ag 3d peak is clearly visible in the survey spectrum. This reveals the presence of Ag in the hybrid films. The intensity of peaks of O (1s) and C (1s) decreases due to formation of the composite structure, as expected. It has to be noted that the shape and position of peaks corresponding to O (1s), C (1s), and Si(2s,2p) does not change with addition of the Ag-NPs which means that the influence of nanoparticles upon the chemical structure of the $(CH_3)_xSiO_y$ film is negligible, at least for the range of used Ag-NPs amount in our work.
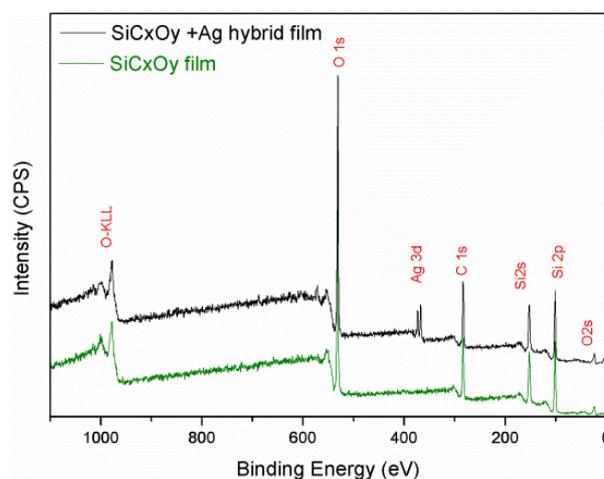
Fig. 3 – XPS spectra of a control film and a hybrid film.

Unfortunately due to the relatively big nanoparticles (100 nm) used in the process, XPS shows a limited measurement capability in our work for Ag quantification and the depth profile. The limitation can be explained by XPS mechanism. XPS spectra are obtained by irradiating a material with a beam of X-rays, while simultaneously measuring the kinetic energy and number of electrons that escape from the top 1 to 10 nm of the material being analyzed. It means that the XPS signal from nanoparticles of a size of 100 nm can be strongly affected by the orientation of nanoparticles inside the film, resulting in a high error in the quantification of the XPS results. Secondly, a depth profile of the sample in terms of XPS quantities can be obtained by combining a sequence of ion gun etch cycles interleaved with XPS measurements from the current surface. The high energy of sputtering ions (such as 4 keV) lead to the unavoidable and uncontrollable matrix effect in a depth profile measurement [14]. This can result in the removal of an entire nanoparticle during sputtering step, leaving a cavity on the surface for the next measurement. Thus, unlike the success in others work on analysis of uniform films of the same chemical structure with small nanoparticles [2, 3, 6–11], the XPS technique obviously has limitations and difficulties when analyzing hybrid films with incorporated Ag-NPs.

3.2. RF-GD-OES MEASUREMENTS

One of the possible techniques to overcome the limitation of XPS method and matrix effect due to high energy of ions is a glow discharge optical emission spectroscopy (RF-GD-OES) used for the analysis of complex samples, mostly metal alloys and ceramics [15, 16].
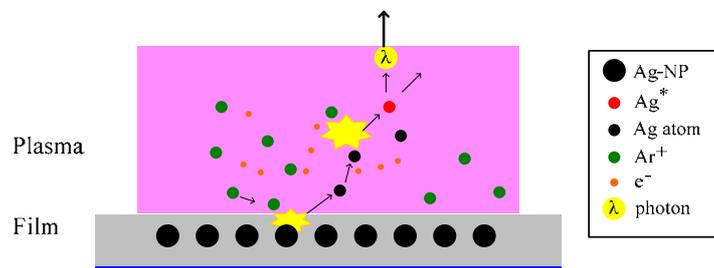
Fig. 4 – Diagrammatic sketch of the Mechanism in the GD-OES.

In the GD-OES, the plasma is initiated when a high potential is applied between the electrodes. The scheme of the technique is presented on Fig. 4. The positive ions (argon ions in the setup) are attracted toward the sample surface, strike the sample surface with an energy of 10–50 eV and cause the release of surface material into the gas phase. Upon entering the gas phase environment of the glow discharge, the sputtered materials are excited by the plasma. Finally, the excited atoms or ions come back to the fundamental energy level, and emit a characteristic photon. The emitted photons, whose energy is characteristic for a chemical element's energy level, are then collected by a spectrometer. This allows to quantify the elemental composition of the material. In comparison with XPS, which measures the sample surface, RF-GD-OES is based on the detection and quantification of sample species within the plasma. Among the advantages of the GD-OES are the simplicity of the technique and the low cost of the analysis.

Table 2

Possible optical emission lines of GD-OES

Element	Peak wavelength	Ai	interference
N	174.267	1.05e+08	As
C	193.093	3.39e+08	–
Ag	328.068	1.4e+08	Ce Mn Rh
Ag	338.289	1.3e+08	–
Si	390.552	1.33e+07	–
Ar	696.543	6.39e+06	–
O	777.196	3.69e+07	–

We used a customer made system with a special RF electrode design developed for analysis of non-conducting samples. The typical emission spectra of RF-GD-OES for a control sample and two hybrid films are presented in Fig. 5. The control sample was deposited without the introduced Ag-NPs. The two hybrid films, sample 1 and sample 2, were obtained with various flow rates of carrying gas for Ag-NPs, 2000 sccm and 1000 sccm respectively. Although the plasma chamber

was pumped to 1×10^{-3} mbar after the placement of samples and flushed by an argon gas flow for three minutes, it is impossible to remove background gases completely. Therefore, the emission signal due to nitrogen impurities is considered as a main component of the background emission. Table 2 shows the ascription of possible peaks of GD-OES in the measurement range for different elements, as suggested in [15].

As shown in the spectra by Fig. 5, emission bands around 337.1 nm and 336 nm are due to the emission from background reactions of nitrogen second positive system N_2(C-B) and the transition of NH(A-X), respectively. A comparison between the control sample (without Ag-NPs introduced into the layer) and the hybrid layers (with Ag-NPs introduced into the film) indicate the existence of two new emission lines for the hybrid samples, at 328.1 and 338.3 nm, respectively. These lines appear due to the transition of 5p → 5s for silver ions. According to the mechanism of the RF-GD-OES, the silver emission lines indicate the presence of silver in the hybrid films. Because of a higher transition probability and stronger emission, the emission at 328.1 nm is considered for further analysis.
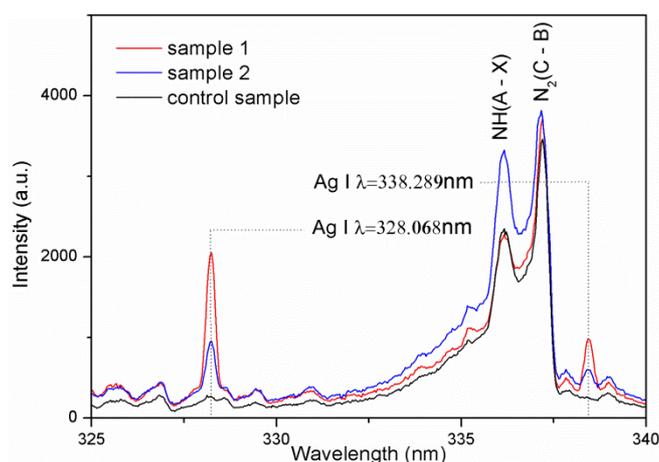

Fig. 5 – Emission spectra of RF-GD-OES. The control sample was obtained without the introduction of Ag-NPs. The sample 1 and sample 2 were deposited with various flow rate of carrying gas, 2000 sccm and 1000 sccm, respectively.

The Ag-NPs distribution in the bulk of the deposited films is determined from the time-resolved measurements of the Ag signal. Due to the sputtering process in the GD-OES, the change of the Ag intensity signal during plasma exposition can reveal the depth profile of the silver in the films. Figure 6 presents the intensity of the emission line as a function of analyzing time. The Ag signal kinetic can be divided into two stages. For the first 75 seconds, the emission from silver ions grows gradually after the ignition of the plasma. This period is considered to be the initialization time after the plasma ignition for the analysis due to the plasma etching, formation of sputtering crater and heating process.

The emission profile is considered to be directly proportional to the Ag density profile. The saturation and almost constant intensity of the Ag line for a sputtering time from 75 s to 210 s demonstrates a uniform distribution of silver in the film.
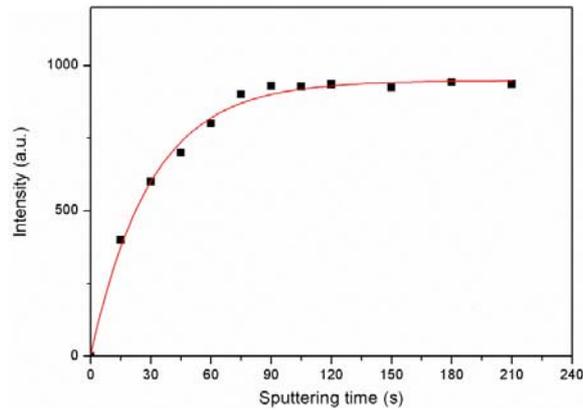

Fig. 6 – Typical kinetic signal of Ag emission line at 328.1 nm as a function of sputtering time.

In glow discharge optical emission spectrometry (GD-OES), the emission intensity of an atomic line is proportional to the product of the concentration of the corresponding element of the sample. For a recorded signal, the emission line from element i is given by [15]:

$$I_i = k_i S_i R_i c_i q_M + b_i,$$

where k_i is the instrumental detection efficiency, S_i is the correction for self-absorption, R_i is the emission yield, c_i is the content of element i, q_i is the sputtering rate, b_i is the background term.
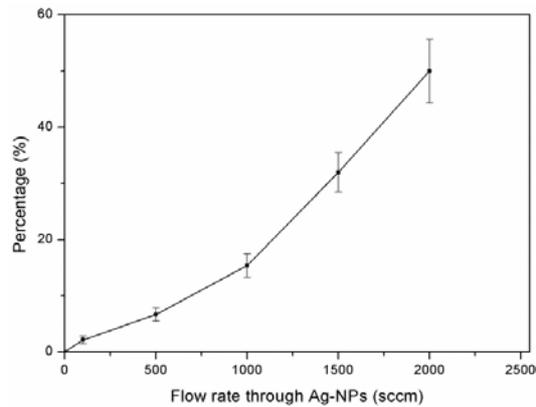

Fig. 7 – Silver content as a function of the flow rate through the Ag-NPs container.

The intensity of Ag signal during the second stage of the sputtering process (from 75 s up to 210 s), as seen in Fig. 6, is used for quantization of the silver in the films in absolute units. The calibration of the RF-GD-OES set-up was carried out by measuring emission intensity of samples as calibration standards, for which the elemental composition is known. The calibration curves, which give the necessary constants in order to determine the sputtered mass per element from the measured emission intensities, are constructed by means of a series of calibration samples. The measurements of Ag content are done for the samples deposited at various gas flow rates passing the Ag-NPs container. As we can see from Fig. 7, the concentration of silver increases significantly with the increase of gas flow through Ag-NPs. It is found that the content of Ag-NPs varies from few percentages to more than 50% which demonstrates the possibility of high control over the composition of the deposited films achieved in the presented system.

4. CONCLUSION

Silver nanoparticles embraced hybrid thin films have been deposited by an atmospheric pressure direct current plasma jet system using TMDSO as organosilicon precursor. Silver nanoparticles were introduced to the plasma jet by a direct nanoparticles feeding system. XPS and RF-GD-OES are used to characterize the films. Both techniques reveal the presence of silvers in the film. Moreover, the results from RF-GD-OES indicate the uniform depth profile of the silver in the films. The content of silver in the film can be varied from few percentages to more than 50% by changing the gas flow through the Ag-NPs container. Further work on the release of silver ion and antibacterial properties of the hybrid films is in progress.

REFERENCES

1. T. S. Sileika, H. D. Kim, P. Maniak and P. B. Messersmith, ACS Appl. Mater. Interfaces, **3**, 4602–4610 (2011).
2. C. Saulou, B. Despax, P. Raynaud, S. Zanna, A. Seyeux, P. Marcus, J.-N. Audinot and M. Mercier-Bonin, Plasma Process. Polym., **9**, 324–338 (2012).
3. S. Lischer, E. Körner, D. J. Balazs, D. Shen, P. Wick, K. Grieder, D. Haas, M. Heuberger and D. Hegemann, J. R. Soc., Interface, **8**, 1019–1030 (2011).
4. N. K. Vu, A. Zille, F. R. Oliveira, N. Carneiro and A. P. Souto, Plasma Process. Polym., **10**, 285–296 (2013).
5. L. Zhao, H. Wang, K. Huo, L. Cui, W. Zhang, H. Ni, Y. Zhang, Z. Wu and P. K. Chu, Biomaterials, **32**, 5706–5716 (2011).
6. X. J. Zan, M. Kozlov, T. J. McCarthy and Z. H. Su, Biomacromolecules, **11**, 1082–1088 (2010).

7. J. Juan, Macromol. Symp., pp. 84–90, 2006.

8. G. Guillemot, B. Despax, P. Raynaud, S. Zanna, P. Marcus, P. Schmitz and M. Mercier-Bonin, Plasma Process. Polym., **5**, 228–238 (2008).

9. C. Saulou, B. Despax, P. Raynaud, S. Zanna, P. Marcus and M. Mercier-Bonin, Appl. Surf. Sci., **256**, S35–S39 (2009).

10. E. Körner, M. H. Aguirre, G. Fortunato, A. Ritter, J. Rühe and D. Hegemann, Plasma Process. Polym., **7**, 619–625 (2010).

11. R. Zimmermann, A. Pfuch, K. Horn, J. Weisser, A. Heft, M. Röder, R. Linke, M. Schnabelrauch and A. Schimanski, Plasma Process. Polym., **8**, 295–304 (2011).

12. G. Lopez-Carballo, L. Higueras, R. Gavara and P. Hernandez-Munoz, J. Agric. Food Chem., **61**, 260–267 (2013).

13. X. Deng, A. Y. Nikiforov, N. De Geyter, R. Morent and C. Leys, Plasma Process. Polym., **10**, 641–648 (2013).

14. A. Holländer, M. Haupt and C. Oehr, Plasma Process. Polym., **4**, 773–776 (2007).

15. T. Nelis and R. Payling, *Glow discharge optical emission spectroscopy: a practical guide*, Royal Society of Chemistry, Cambridge, 2003.

16. M. R. Winchester and R. Payling, Spectrochim. Acta, Part B, **59**, 607–666 (2004).